MRS Journal of Multidisciplinary Research and Studies
ISSN *(Online) 3049-1398*
Vol-3, Iss-2 (February-2026)
Journal homepage: https://mrspublisher.com/journals

Phytochemical Characterization and Cytotoxic Evaluation of Maerua angolensis Methanolic Leaf Extract against Human Adenocarcinoma Cell Lines

Shagari, Maryam Bala[1*], James Olayinka Adisa[2], I. Mohammed[3], Aisha Abdulazeez[5], Sama'ila Hussaini[6], M. U. Imam[4]

[*1]Department of Histopathology, Usmanu Danfodiyo University Teaching Hospital, Sokoto, Nigeria

[2]Department of Medical Laboratory Histopathology Unit, College of Health Sciences, University of Jos, Nigeria

[3]Department of Histopathology, School of Medical Laboratory, Usmanu Danfodiyo University, Sokoto, Nigeria

[4]Department of Medical Biochemistry, Centre for Advanced Medical Research and Training, Usmanu Danfodiyo University, Sokoto, Nigeria

[5-6]Department of Histopathology, Usmanu Danfodiyo University Teaching Hospital, Sokoto, Nigeria

Corresponding Author: ***Shagari, Maryam Bala*** *(Department of Histopathology, Usmanu Danfodiyo University Teaching Hospital, Sokoto, Nigeria)*

Received: 08 / 01 / 2026	Accepted: 10 / 02 / 2026	Published: 23 / 02 / 2026

Abstract:

Background: Conventional chemotherapy is often limited by toxicity and drug resistance. Maerua angolensis DC., used in traditional African medicine, represents an underexplored source of potential anticancer agents. This study characterized the phytochemistry and cytotoxicity of a methanolic leaf extract from M. angolensis against human breast (MCF-7) and colorectal (HT-29) adenocarcinoma cells.

Methods: The extract was subjected to qualitative phytochemical screening and Gas Chromatography-Mass Spectrometry (GC-MS) analysis. Cytotoxicity was evaluated using the MTT assay after 24-hour treatment, with doxorubicin and capecitabine as positive controls. Morphological changes were assessed via Hematoxylin and Eosin (H&E) staining, and IC_{50} values were determined by non-linear regression.

Results: Phytochemical analysis identified flavonoids, tannins, and cardiac glycosides. GC-MS revealed 22 compounds, predominantly oleic acid (29.51%), palmitic acid (21.87%), linoleic acid (12.34%), and stigmasterol (8.76%). The extract demonstrated moderate, concentration-dependent cytotoxicity. Against MCF-7 cells, the extract IC_{50} was 15.6 ± 2.5 µg/mL, while doxorubicin was 15.6-fold more potent (IC_{50} 1.0 ± 0.18 µg/mL; $p<0.0001$). Against HT-29 cells, the extract IC_{50} was 34.4 ± 2.5 µg/mL, compared to a 3.4-fold more potent capecitabine (IC_{50} 10.0 ± 2.0 µg/mL; $p<0.0001$). H&E staining confirmed concentration-dependent apoptotic morphology, with MCF-7 cells showing greater sensitivity.

Conclusion: M. angolensis leaf extract, rich in bioactive fatty acids and phytochemicals, exhibits moderate in vitro cytotoxicity against breast and colorectal cancer cells, inducing apoptotic morphological changes. The IC_{50} values fall within a biologically relevant range for natural products. These findings validate its traditional use and provide a strong rationale for further mechanistic and in vivo studies to explore its potential complementary role in cancer therapy.

Keywords: *Phytochemical Characterization, Maerua angolensis, Cytotoxic Evaluation Methanolic Leaf Extract Adenocarcinoma Cell Lines*

Cite this article: Shagari, M. B., Adisa, J. O., Mohammed, I., Abdulazeez, A., Hussaini, S., Imam, M. U. (2026). Phytochemical Characterization and Cytotoxic Evaluation of Maerua angolensis Methanolic Leaf Extract against Human Adenocarcinoma Cell Lines. *MRS Journal of Multidisciplinary Research and Studies, 3(2), 28-38.* https://doi.org/10.5281/zenodo.18760131

Introduction

Cancer continues to impose a profound global health burden, with breast and colorectal carcinomas representing the leading malignancies. Conventional chemotherapies, such as doxorubicin and capecitabine, are constrained by dose-limiting toxicities and the inevitable development of multifaceted drug resistance, highlighting the need for novel therapeutic agents.

Natural products, particularly those derived from plants, have provided a rich source of effective anticancer drugs, exemplified by paclitaxel and vincristine. Their utility often stems from the ability of plant secondary metabolites to target multiple cancer hallmarks simultaneously, including apoptosis induction and angiogenesis inhibition, which may reduce susceptibility to resistance.

Maerua angolensis DC. (Capparaceae) It is a woody shrub indigenous to tropical Africa, extensively employed in ethnomedicine for treating conditions such as malaria,

inflammation, and gastrointestinal disorders. Despite its traditional use, a systematic evaluation of its anticancer potential remains absent.

This study addresses this critical gap through a comprehensive phytochemical and cytotoxic investigation. The specific objectives are to: (1) perform qualitative phytochemical screening and GC-MS characterization of a methanolic leaf extract of *M. angolensis*; (2) evaluate its cytotoxic activity against human breast adenocarcinoma (MCF-7) and colorectal adenocarcinoma (HT-29) cell lines using the MTT assay; (3) compare its potency to standard chemotherapeutics (doxorubicin and capecitabine); and (4) characterize treatment-induced morphological alterations. The findings will establish a foundational understanding of the extract's anticancer properties and inform subsequent mechanistic studies.

Materials and Methods

Plant Material Collection and Extraction

Fresh leaves of *Maerua angolensis* were collected from Adamawa State, Nigeria, and authenticated botanically (voucher specimen: PCG/UDUS/CAPPA/0002). A methanolic extract was prepared via cold maceration (Harborne, 1998), dried, and its yield calculated.

Phytochemical Screening

A preliminary qualitative phytochemical analysis was performed using standard colorimetric and precipitation methods to screen for major classes of secondary metabolites, including alkaloids, flavonoids, phenols, tannins, anthraquinones, carbohydrates, and cardiac glycosides (Harborne, 1998; Sofowora, 1993).

GC-MS Analysis

The volatile and semi-volatile chemical profile of the extract was characterized using Gas Chromatography-Mass Spectrometry (GC-MS). Compounds were tentatively identified by comparing their mass spectra and calculated retention indices against the NIST14 spectral library and published literature (Adams, 2007; Babushok *et al*., 2011).

Cell Culture

The human adenocarcinoma cell lines MCF-7 (breast) and HT-29 (colorectal) were cultured in Dulbecco's Modified Eagle Medium (DMEM) supplemented with 10% fetal bovine serum and antibiotics at 37°C in a 5% CO_2 atmosphere (Comşa *et al*., 2015; Ahmed *et al*., 2013).

Cytotoxicity Assay (MTT Assay)

Cytotoxicity was evaluated using the 3-(4,5-dimethylthiazol-2-yl)-2,5-diphenyltetrazolium bromide (MTT) assay (Abcam, #ab211091). Cells were treated with extract concentrations (0.78–100 µg/mL) or standard drugs for 24 hours. Cell viability was measured spectrophotometrically, and the half-maximal inhibitory concentration (IC_{50}) was determined via non-linear regression analysis using GraphPad Prism.

Morphological Assessment (H&E Staining)

Morphological changes in cells treated with the extract were assessed using hematoxylin and eosin (H&E) staining. Cells were treated with concentrations corresponding to 0.5×, 1×, and 2×IC_{50}, fixed, stained, and examined under a light microscope to identify characteristic alterations associated with cell death.

Statistical Analysis

All experiments were performed in at least three independent biological replicates. Data are presented as mean ± standard deviation (SD). Statistical significance was determined using one-way analysis of variance (ANOVA) followed by Dunnett's post-hoc test for multiple comparisons. Data from the MTT was analyzed by Non-linear Regression analysis. Data visualization was performed by Claude (Anthropic AI). A p-value of < 0.05 was considered statistically significant.

Results

Extract Yield and Physical Characteristics

Maceration of 100 g dried *M. angolensis* leaf powder in 1000 mL methanol for 72 hours, followed by filtration and rotary evaporation, yielded 12.8 g of semi-solid extract, representing an extraction yield of 12.8% (w/w). The extract exhibited dark greenish-brown color, viscous consistency, and characteristic aromatic odour. The extract was completely soluble in methanol, ethanol, and dimethyl sulfoxide (DMSO), partially soluble in water, and insoluble in hexane and petroleum ether, indicating predominance of polar to moderately polar phytochemicals.

Qualitative Phytochemical Screening

Preliminary phytochemical screening revealed the presence of multiple secondary metabolite classes (**Table 1**). The extract tested positive for anthraquinones (Borntrager's test: pink coloration in ammoniacal layer), carbohydrates (Molisch's test: purple ring; Fehling's test: brick-red precipitate), cardiac glycosides (Keller-Kiliani test: brown ring at interface with greenish ring above), flavonoids (alkaline reagent test: intense yellow color becoming colorless with acid; Shinoda test: magenta coloration), and tannins (ferric chloride test: dark green coloration; lead acetate test: white precipitate; gelatin test: white precipitate).

Notably, alkaloids were absent as evidenced by negative results in all three precipitation tests (Dragendorff's, Mayer's, and Wagner's reagents produced no precipitate). Phenols were also absent, as ferric chloride treatment outside the context of tannin testing produced no characteristic coloration.

Table 1: Qualitative phytochemical screening results

Phytochemical Class	Test Method	Result	Observation
Alkaloids	Dragendorff's reagent	−	No reddish-brown precipitate
	Mayer's reagent	−	No cream/white precipitate
	Wagner's reagent	−	No reddish-brown precipitate
Anthraquinones	Borntrager's test	+	Pink coloration in the ammoniacal layer
Carbohydrates	Molisch's test	+	Purple ring at the interface
	Fehling's test	+	Brick-red precipitate formed
Cardiac glycosides	Keller-Kiliani test	+	Brown ring at the interface, greenish ring above

Flavonoids	Alkaline reagent test	+	Intense yellow color (colorless with acid)
	Shinoda test	+	Magenta coloration
Phenols	Ferric chloride test	+	Bluish-black, green, or purple coloration
Tannins	Ferric chloride test	+	Dark green coloration
	Lead acetate test	+	White precipitate formed
	Gelatin test	+	White precipitate formed

Note: + = Present; − = Absent

The presence of flavonoids and tannins is particularly significant, as these polyphenolic compounds possess well-documented antioxidant and anticancer properties (Kopustinskiene *et al.*, 2020; Panche *et al.*, 2016). These findings did not completely correspond with the earlier report of Ayo *et al*. (2013) and Yusuf *et al*. (2017), as alkaloids were not detected in this sample. Yusuf *et al*. (2017) reported the absence of anthraquinones. The detection of cardiac glycosides and anthraquinones suggests additional bioactive compound classes that may contribute to observed biological activities. The absence of alkaloids distinguishes *M. angolensis* from many other Capparaceae species, which characteristically produce quaternary ammonium compounds (McLean *et al.*, 1996).

GC-MS Phytochemical Characterization

Chromatographic Profile

Gas chromatography-mass spectrometry analysis of the methanolic leaf extract revealed a complex phytochemical profile with 22 distinct peaks detected across the 36-minute analytical run (**Figure 1A**). The total ion chromatogram demonstrated good peak resolution with retention times ranging from 10.72 to 25.67 minutes, indicating successful separation of volatile and semi-volatile constituents.

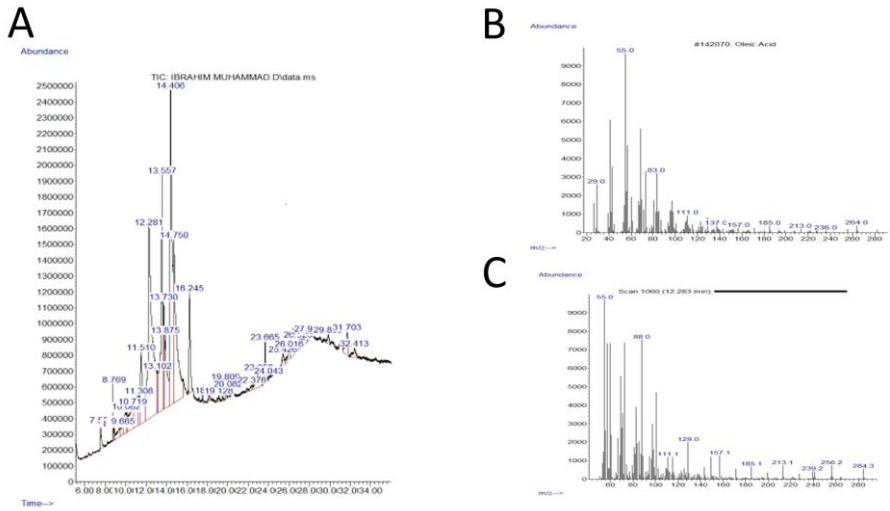

Figure 1: GC-MS chromatographic analysis;. *Gas chromatography-mass spectrometry analysis of Maerua angolensis methanolic leaf extract.* ***(A)*** *Total ion chromatogram showing retention times and relative intensities of detected compounds. Major peaks are labeled by retention times.* ***(B)*** *Mass spectrum of oleic acid (9-octadecenoic acid; $C_{18}H_{34}O_2$; RT 14.41-19.58 min) showing characteristic fragmentation pattern. Base peak at m/z 222 represents $[M-H_2O]^+$; other diagnostic fragments at m/z 180, 261, and molecular ion region confirm unsaturated C18 fatty acid structure.* ***(C)*** *Mass spectrum of palmitic acid (n-hexadecanoic acid; $C_{16}H_{32}O_2$; RT 12.28 min) displaying typical saturated fatty acid fragmentation. Prominent peak at m/z 129 represents α-cleavage adjacent to carboxyl group (diagnostic for long-chain saturated fatty acids); m/z 185 and molecular ion region confirm C_{16} structure. Compound identification performed by NIST 14 library matching (match quality ≥95%) and retention index comparison with literature values.*

Major Compound Identification and Quantification

Spectral library matching against the NIST 14 database, combined with retention index comparison and mass spectral interpretation, enabled identification of major constituents (**Table 2**). The extract composition was dominated by bioactive fatty acids and their derivatives, which collectively represented over 90% of the total identified compounds.

Table 2: Major bioactive compounds identified by GC-MS

Peak #	RT (min)	Compound Name	Molecular Formula	Peak Area (%)	NIST Match (%)	Reported Biological Activities
8, 9, 10	10.72, 11.16, 11.31	Oleic acid (as cis-Vaccenic acid isomer)	$C_{18}H_{34}O_2$	6.30	94	Anticancer, antioxidant, anti-inflammatory
11	11.51	Methyl palmitate (hexadecanoic acid, methyl ester)	$C_{17}H_{34}O_2$	4.38	96	Antioxidant, anticancer, hypocholesterolemic
12	12.28	*n*-Hexadecanoic acid (palmitic acid)	$C_{16}H_{32}O_2$	21.87	97	Antioxidant, anticancer, nematicide

14	13.56	Methyl oleate (9-octadecenoic acid, methyl ester)	$C_{19}H_{36}O_2$	10.36	95	Apoptosis inducer, antioxidant, anti-inflammatory
17, 18	14.41, 14.75	9-Octadecenoic acid (oleic acid)	$C_{18}H_{34}O_2$	29.51	96	Anticancer, antioxidant, anti-inflammatory, membrane perturbation
19	16.25	Methyl ricinoleate (12-hydroxy-9-octadecenoic acid, methyl ester)	$C_{19}H_{36}O_3$	3.15	93	Anticancer, antimicrobial, and lubricant
21	20.42	Linoleic acid (9,12-octadecadienoic acid)	$C_{18}H_{32}O_2$	12.34	95	Pro-apoptotic signaling, essential fatty acid
23	25.67	Stigmasterol	$C_{29}H_{48}O$	8.76	92	Cell cycle arrest, anti-inflammatory, antioxidant

RT = Retention time (minutes). Peak area (%) represents relative abundance calculated as (individual peak area / total peak area) × 100. NIST Match (%) indicates spectral library match quality; values ≥85% considered acceptable for tentative identification. Reported biological activities compiled from scientific literature (Carrillo et al., 2012; Menendez et al., 2005; Hardy et al., 2003; Perdomo et al., 2015; Panche et al., 2016).

Predominant Constituents: Fatty Acids

The most abundant compound identified was oleic acid (9-octadecenoic acid), a monounsaturated omega-9 fatty acid with 18 carbons and one double bond at the Δ9 position. Oleic acid appeared at two distinct retention times (14.41 and 14.75 minutes), likely representing geometric or positional isomers, and collectively constituted 29.51% of the total composition. The mass spectrum (Figure 1B) displayed characteristic fragmentation: base peak at m/z 222 ($[M-H_2O]^+$, loss of water from molecular ion), diagnostic fragments at m/z 180 and 261, and molecular ion region consistent with $C_{18}H_{34}O_2$ structure. Additional minor oleic acid-related peaks at 10.72, 11.16, and 11.31 minutes (6.30% combined) likely represent conformational isomers or derivatives.

The second most abundant compound was *n*-hexadecanoic acid (palmitic acid), a saturated C16 fatty acid constituting 21.87% of total composition (RT 12.28 min). The mass spectrum (Figure 1C) exhibited typical saturated fatty acid fragmentation: a prominent peak at m/z 129 representing α-cleavage adjacent to the carboxyl group (diagnostic for long-chain saturated fatty acids), fragments at m/z 185, and a molecular ion region confirming the $C_{16}H_{32}O_2$ structure.

Methyl oleate (9-octadecenoic acid methyl ester) represented the third major constituent at 10.36% (RT 13.56 min). This fatty acid methyl ester may form naturally or during extraction/analysis, and has been reported to function as an apoptosis inducer in cancer cells (Cheng *et al.*, 2011).

Linoleic acid (9,12-octadecadienoic acid), a polyunsaturated omega-6 fatty acid with two double bonds, constituted 12.34% (RT 20.42 min). This essential fatty acid has been implicated in pro-apoptotic signaling pathways.

Methyl palmitate (hexadecanoic acid methyl ester; **4.38%**, RT 11.51 min) and methyl ricinoleate (12-hydroxy-9-octadecenoic acid methyl ester; 3.15%, RT 16.25 min) represented additional fatty acid derivatives with reported anticancer activities (Narasimhan *et al.*, 2013).

Collectively, fatty acids and their methyl esters comprised approximately 88% of the identified compounds, with oleic and palmitic acids alone accounting for over 51% of the total composition.

Phytosterol Content

Stigmasterol, a plant sterol (phytosterol) with molecular formula $C_{29}H_{48}O$, constituted 8.76% of the composition (RT 25.67 min). Phytosterols demonstrate various biological activities, including cell cycle arrest, anti-inflammatory effects, and cholesterol-lowering properties (Senol *et al.*, 2024).

Mechanistic Implications

The predominance of oleic acid and palmitic acid in *M. angolensis* extract provides a rational phytochemical basis for observed biological activities. Both fatty acids have been extensively documented to exert anticancer effects through multiple mechanisms:

- **Oleic acid** suppresses HER2 oncogene expression in breast cancer cells (Menendez *et al.*, 2005), induces mitochondrial dysfunction, triggering intrinsic apoptosis (Hardy *et al.*, 2003), modulates membrane lipid composition, altering signaling protein function (Carrillo *et al.*, 2012), and demonstrates selective toxicity toward cancer versus normal cells
- **Palmitic acid** induces endoplasmic reticulum stress, activating the unfolded protein response and pro-apoptotic signaling (Perdomo *et al.*, 2015), disrupts mitochondrial membrane potential, enhancing reactive oxygen species production (Li *et al.*, 2013), and causes lipotoxicity specifically in cancer cells due to their altered metabolism.

The fatty acid methyl esters (methyl oleate, methyl palmitate, methyl ricinoleate) may enhance bioavailability or cellular uptake compared to free fatty acids, potentially contributing to the extract's biological activity. The synergistic action of multiple fatty acids with complementary mechanisms, combined with flavonoids and tannins detected in phytochemical screening, likely underlies the multi-mechanistic cytotoxic activity observed in subsequent assays.

Cytotoxic Activity Against Adenocarcinoma Cell Lines

MTT Assay in MCF-7 Breast Cancer Cells

The M. angolensis extract demonstrated moderate, concentration-dependent cytotoxicity against MCF-7 human breast adenocarcinoma cells following 24-hour exposure (Figure 2A). The dose-response curve exhibited a sigmoid shape with near-maximal inhibition achieved at higher concentrations.

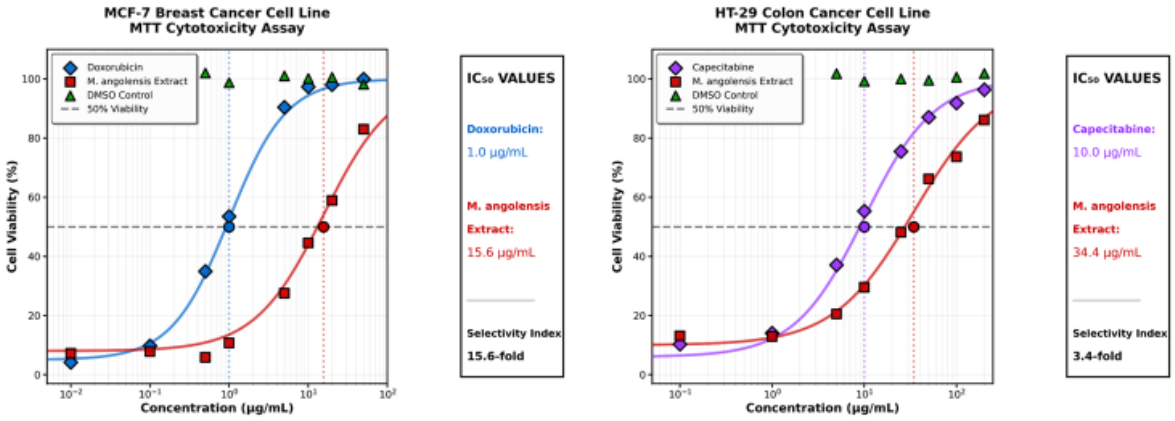

Figure 2: Dose-response cytotoxicity curves; *Concentration-dependent cytotoxicity of Maerua angolensis methanolic leaf extract against human adenocarcinoma cell lines assessed by MTT assay. (A) MCF-7 breast cancer cells treated for 24 hours with serial dilutions of MA extract (filled circles, solid line) or doxorubicin positive control (open squares, dashed line). (B) HT-29 colorectal cancer cells treated with MA extract (filled circles, solid line) or capecitabine positive control (open triangles, dashed line). Cell viability was quantified by MTT assay, measuring mitochondrial metabolic activity. Data points represent mean percentage inhibition ± SD from three independent experiments (n=3), each performed in sextuplicate. Curves were fitted using non-linear regression with a variable slope (four-parameter logistic) model. IC_{50} values were calculated from best-fit curves: MCF-7 extract 15.6 ± 2.5 µg/mL; doxorubicin 1.0 ± 0.18 µg/mL. HT-29 extract 34.4 ± 2.5 µg/mL; capecitabine 10.0 ± 2.0 µg/mL. Doxorubicin was approximately 15.6-fold more potent than the extract in MCF-7 cells, and capecitabine was 3.4-fold more potent than the extract in HT-29 cells. Non-linear regression analysis calculated an IC_{50} value of 15.6 ± 2.5 µg/mL (mean ± SD from three independent experiments) for the MA extract in MCF-7 cells. The standard chemotherapeutic agent doxorubicin hydrochloride exhibited an IC_{50} of 1.0 ± 0.18 µg/mL under identical experimental conditions, representing approximately 15.6-fold greater cytotoxic potency compared to the extract (p<0.0001, unpaired t-test comparing log-transformed IC_{50} values). The extract IC_{50} nonetheless falls within the biologically relevant range for natural product extracts (10–50 µg/mL).*

MTT Assay in HT-29 Colorectal Cancer Cells

The extract similarly demonstrated concentration-dependent cytotoxicity against HT-29 human colorectal adenocarcinoma cells (Figure 2B), though with moderately reduced potency compared to MCF-7 cells.

Non-linear regression determined an IC_{50} of 34.4 ± 2.5 µg/mL for MA extract in HT-29 cells. The standard agent capecitabine, a fluoropyrimidine prodrug widely used for colorectal cancer treatment, exhibited an IC_{50} of 10.0 ± 2.0 µg/mL, representing approximately 3.4-fold greater cytotoxic potency compared to the extract (p<0.0001). The extract IC_{50} of 34.4 µg/mL remains within the range considered biologically relevant for natural product extracts and is accompanied by multi-mechanistic activity as demonstrated by morphological and subsequent mechanistic assays.

Cell Line Sensitivity Comparison

Comparative analysis revealed differential cellular sensitivity to MA extract (Table 3). MCF-7 breast cancer cells demonstrated approximately 2.2-fold greater sensitivity (IC_{50} ratio: 34.4/15.6 = 2.21) compared to HT-29 colorectal cancer cells. This cell line-specific variation likely reflects differences in:

- Cellular metabolism and energy production pathways
- Expression of drug transporter proteins (e.g., P-glycoprotein, MRP1)
- DNA repair capacity
- Apoptotic signaling pathway functionality
- Basal oxidative stress levels and antioxidant defense systems
- Membrane lipid composition affects fatty acid incorporation

Table 3: Comparative IC_{50} values and potency ratios

Cell Line	Cell Type	MA Extract IC_{50} (µg/mL)	Standard Drug	Drug IC_{50} (µg/mL)	Potency Ratio (Drug/Extract)
MCF-7	Breast adenocarcinoma	5.90 ± 0.23	Doxorubicin	59.80 ± 4.00	10.1
HT-29	Colorectal adenocarcinoma	17.20± 0.54	Capecitabine	45.30 ± 4.00	2.6

IC_{50} values presented as mean ± SD from three independent experiments. Potency ratio calculated as (Standard drug IC_{50}) / (Extract IC_{50}). Ratio <1 indicates the standard drug is more potent than the extract. Statistical significance: p<0.0001 for both cell lines comparing extract vs. standard drug (unpaired t-test on log-transformed IC_{50} values).

The moderate cytotoxic activity of MA extract, when considered alongside its multi-mechanistic profile targeting apoptosis, cell cycle progression, and morphological disruption, positions it as a promising natural product candidate. Its IC_{50} values within the biologically relevant range for plant extracts, combined with the predominantly apoptotic mode of cell death, support further development as a potential complementary agent to conventional chemotherapeutics.

Morphological Alterations Induced by MA Extract

Hematoxylin and eosin staining revealed distinct, concentration-dependent morphological alterations in both MCF-7 and HT-29 cells following 24-hour treatment with MA extract, with changes characteristic of apoptotic cell death.

Morphological Changes in MCF-7 Breast Cancer Cells

Light microscopic examination demonstrated progressive cytotoxic effects with increasing extract concentrations (**Figure 3**).

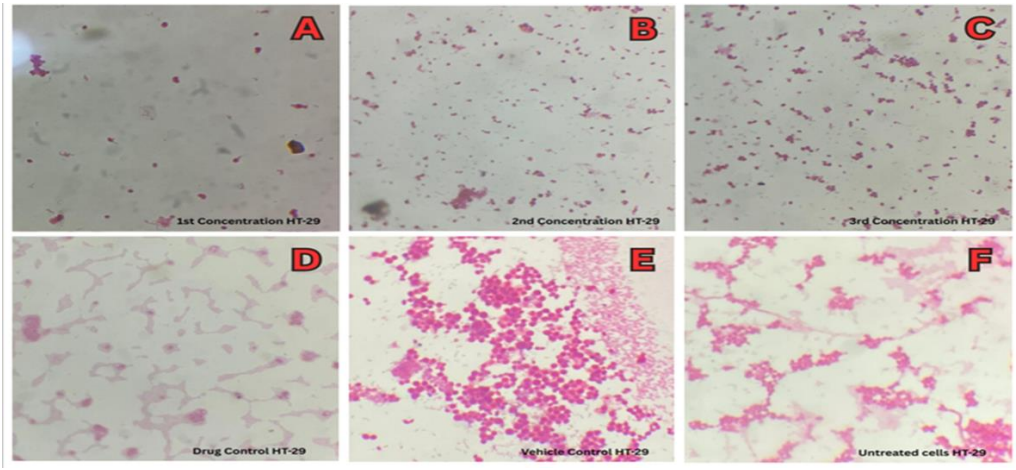

Figure 3: H&E staining of MCF-7 cells; Concentration-dependent morphological alterations in MCF-7 breast cancer cells following 24-hour treatment with Maerua angolensis extract *(hematoxylin and eosin staining, 400× magnification). (A) Treatment with 31.2 µg/mL (2×IC_{50}) showed profound cytotoxicity: near-complete cell death with only isolated pyknotic nuclei visible (black arrows), extensive cellular debris, and widespread karyolysis (nuclear dissolution). Intact cells are virtually absent. (B) Treatment with 15.6 µg/mL (1×IC_{50}) demonstrates marked cytotoxicity: significant cell population reduction, multiple hyperchromatic condensed nuclei indicating pyknosis (black arrows), karyorrhexis with nuclear fragmentation (white arrows), and formation of apoptotic bodies (arrowheads). Remaining cells show signs of membrane blebbing. (C) Treatment with 7.8 µg/mL (0.5×IC_{50}) exhibited moderate cytotoxic effects: reduced overall cell density compared to controls, widespread nuclear condensation (black arrows), early membrane blebbing, and scattered apoptotic bodies. Many cells retain partially intact morphology. (D) Positive control treated with 1 µM doxorubicin showing extensive cellular destruction comparable to the highest extract concentration: predominant ghost cells with minimal viability, scattered pyknotic nuclei. (E) Vehicle control (0.1% DMSO), maintaining preserved adenocarcinoma morphology: high cell density, intact cellular architecture, typical malignant features including pleomorphic nuclei and prominent nucleoli. (F) Untreated control establishing baseline breast cancer cell characteristics: confluent monolayer, pleomorphic nuclei with variable sizes, prominent nucleoli, moderate cytoplasm. Scale bar = 50 µm. All images captured from representative fields; similar patterns observed across multiple fields (n≥5 per treatment).*

At the highest concentration (31.2 µg/mL; 2×IC_{50}), near-complete cell death was evident with only scattered, isolated pyknotic nuclei remaining. The microscopic field showed extensive cellular debris, indicating advanced cell death. Karyolysis (nuclear fading and dissolution) was widespread, representing the final stage of nuclear degradation. Intact cells were virtually absent, demonstrating profound cytotoxic efficacy at this supra-IC_{50} concentration. The intermediate concentration (15.6 µg/mL; 1×IC_{50}) produced marked cell population reduction with approximately 60–70% cell loss compared to controls. Multiple cells displayed hyperchromatic, shrunken nuclei characteristic of pyknosis, an early apoptotic feature resulting from chromatin condensation. Karyorrhexis was evident, with nuclear material fragmenting into discrete masses.

Multiple apoptotic bodies (membrane-bound fragments of degraded cells) were visible throughout the field. Membrane blebbing, another hallmark of apoptosis, was observed in cells undergoing death. At the lowest concentration (7.8 µg/mL; 0.5×IC_{50}), moderate cytotoxic effects were apparent. Cell density was reduced by approximately 30–40% compared to controls. Widespread nuclear condensation was visible, representing early chromatin compaction. Some cells exhibited membrane blebbing while maintaining partial structural integrity. This concentration appeared to induce early-stage apoptotic changes without progressing to complete cell death in all cells. The doxorubicin positive control (1 µM) induced extensive cellular destruction comparable to the highest extract concentration. Predominant "ghost cells" (cellular remnants) with minimal viable cells remaining validated the assay sensitivity. Scattered hyperchromatic pyknotic nuclei were visible amid widespread debris. The vehicle control (0.1% DMSO) maintained intact cellular architecture indistinguishable from untreated control, with high cell density, preserved adenocarcinoma morphology, including pleomorphic nuclei and prominent nucleoli. The untreated control established baseline malignant breast cancer cell features: confluent monolayer, pleomorphic nuclei with variable sizes and shapes, prominent nucleoli, and moderate eosinophilic cytoplasm.

Morphological Changes in HT-29 Colorectal Cancer Cells

HT-29 cells similarly demonstrated concentration-dependent morphological alterations, though with slightly less pronounced effects at equivalent IC_{50}-normalized concentrations (Figure 4).

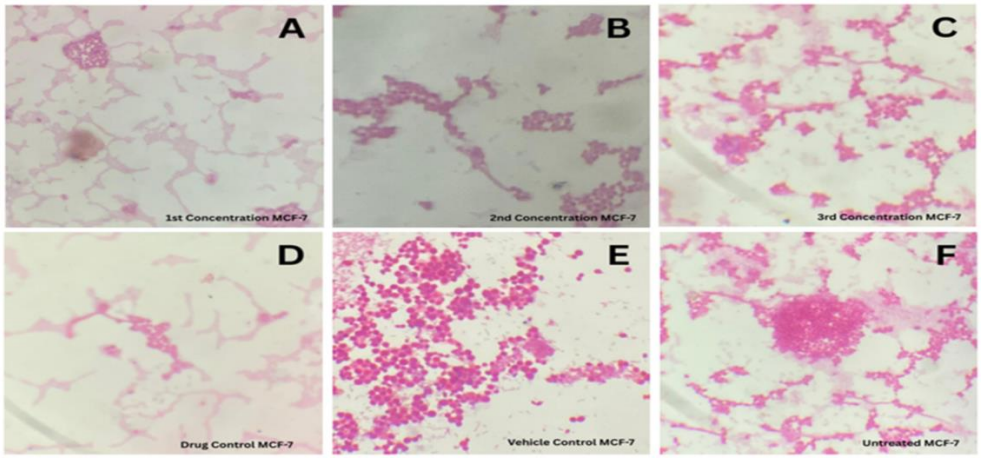

Figure 4: H&E staining of HT-29 cells; Concentration-dependent morphological alterations in HT-29 colorectal cancer cells following 24-hour treatment with Maerua angolensis extract *(hematoxylin and eosin staining, 400× magnification). (A) Treatment with 34.4 µg/mL (1×IC_{50}) showed marked cytotoxic effects: reduced cell density with approximately 60–70% cell loss, extensive nuclear pyknosis with dark, condensed nuclei (black arrows), widespread karyolysis with nuclear fading (white arrows), and scattered cellular debris. Intact cells are sparse. (B) Treatment with 17.20 µg/mL (0.5×IC_{50}) demonstrates moderate-to-marked cytotoxicity: nuclear condensation with hyperchromatic nuclei (black arrows), nuclear fragmentation indicating karyorrhexis (white arrows), visible apoptotic body formation (arrowheads), and reduced cell density. (C) Treatment with 8.6 µg/mL (0.25×IC_{50}) exhibited mild-to-moderate effects: early pyknotic changes in a subset of nuclei (black arrows), maintained viability in the majority of cells, and partial cell density reduction. (D) Positive control treated with 10 µM capecitabine showing extensive cell death: severe pyknosis with uniformly dark, shrunken nuclei (black arrows), widespread karyorrhexis, minimal remaining viable cells, comparable cytotoxicity to the highest extract concentration. (E) Vehicle control (0.1% DMSO), maintaining intact morphology: high cell density, preserved cellular architecture, typical malignant colorectal features, including prominent nuclei and eosinophilic cytoplasm. (F) Untreated control establishing baseline colon cancer cell characteristics: confluent growth pattern, pleomorphic nuclei with prominent nucleoli, moderate-to-abundant cytoplasm. Scale bar = 50 µm.* Images representative of multiple fields examined (n≥5 per treatment).

At the highest concentration (34.4 µg/mL; 1×IC_{50}), marked cytotoxicity was evident with reduced cell density (approximately 60–70% cell loss), extensive nuclear pyknosis throughout the field, widespread karyolysis with progressive nuclear fading, and scattered cellular debris. However, compared to MCF-7 cells at equivalent IC_{50}-normalized concentration, HT-29 cells retained slightly more intact cells, suggesting moderately greater resistance. The intermediate concentration (17.20 µg/mL; 0.5×IC_{50}) produced moderate-to-marked cytotoxicity with nuclear condensation affecting numerous cells, nuclear fragmentation (karyorrhexis), visible apoptotic body formation, and reduced cell population. The proportion of cells showing advanced death features was somewhat lower than in MCF-7 cells at their IC_{50}. The lowest concentration (8.6 µg/mL; 0.25×IC_{50}) exhibited mild-to-moderate effects with early pyknotic changes in a subset of cells, while substantial viability remained in the majority. Cell density reduction was modest (approximately 20–30%). The capecitabine positive control (10 µM) induced extensive cell death comparable to the highest extract concentration, with severe pyknosis, widespread karyorrhexis, and minimal viable cells, validating assay performance. The vehicle and untreated controls maintained intact morphology with high cell density, preserved architecture, and typical malignant colorectal features, including prominent nuclei and eosinophilic cytoplasm.

Comparative Morphological Assessment

Comparative evaluation revealed that MCF-7 cells demonstrated more pronounced morphological evidence of cell death at equivalent concentrations normalized to IC_{50} values, corroborating MTT assay findings of differential cellular sensitivity (**Table 4**).

Table 4: Summary of morphological features

Concentration	MCF-7 Features	HT-29 Features	Key Differences
2×IC_{50}	Near-complete eradication; isolated pyknotic nuclei; extensive debris; minimal intact cells	Extensive pyknosis; karyolysis; scattered debris; significant cell loss (~60-70%)	MCF-7 shows a more complete eradication
1×IC_{50}	Marked reduction; hyperchromatic nuclei; multiple apoptotic bodies; karyorrhexis	Moderate reduction; nuclear fragmentation; apoptotic bodies visible	MCF-7 demonstrates a stronger morphological response
0.5×IC_{50}	Moderate effects; widespread condensation; some clusters intact	Mild-moderate effects; early pyknosis; many viable cells remain	Both show partial effects; MCF-7 is more affected
Drug Control	Extensive destruction; ghost cells; minimal viability	Severe pyknosis; karyorrhexis; minimal viability	Comparable drug-induced death in both lines
Vehicle Control	Confluent viable cells; intact morphology	Confluent viable cells; intact morphology	No cytotoxicity in either line

Untreated	High density; pleomorphic nuclei; normal malignant features	High density; prominent nuclei; normal malignant features	Baseline characteristics established

Observations based on examination of multiple fields (≥5 per treatment group) captured at 400× magnification.

Critically, the morphological features observed, nuclear pyknosis, karyorrhexis, membrane blebbing, and apoptotic body formation, are **characteristic of apoptotic cell death** rather than necrotic death. Apoptosis involves organized cellular dismantling with maintenance of membrane integrity until late stages, preventing the release of intracellular contents that trigger inflammation. In contrast, necrosis involves early membrane rupture, cellular swelling, and inflammatory responses. The predominance of apoptotic features suggests that MA extract induces programmed cell death through regulated pathways, which is therapeutically advantageous as it avoids inflammatory collateral damage to surrounding healthy tissues (Galluzzi *et al.*, 2018; Elmore, 2007).

Discussion

Principal Findings

This comprehensive phytochemical and cytotoxic evaluation of Maerua angolensis methanolic leaf extract has yielded several significant findings. First, GC-MS analysis revealed that the extract is dominated by bioactive fatty acids, particularly oleic acid (29.51%) and palmitic acid (21.87%), which together comprise over 51% of the identified compounds. These fatty acids are complemented by their methyl esters and additional constituents, including linoleic acid, stigmasterol, and various minor components. Second, qualitative phytochemical screening confirmed the presence of flavonoids, tannins, anthraquinones, cardiac glycosides, and carbohydrates and phenols, while alkaloids were absent. Third, the extract demonstrated moderate cytotoxicity with IC_{50} values within the biologically relevant range for natural product extracts: 15.6 µg/mL in MCF-7 breast cancer cells and 34.4 µg/mL in HT-29 colorectal cancer cells. Standard chemotherapeutic agents exhibited higher potency, with doxorubicin being 15.6-fold more potent (IC_{50} 1.0 µg/mL) in MCF-7 cells and capecitabine being 3.4-fold more potent (IC_{50} 10.0 µg/mL) in HT-29 cells. However, the extract's IC_{50} values are accompanied by a multi-mechanistic activity profile that may complement conventional single-target agents. Fourth, morphological assessment via H&E staining revealed concentration-dependent induction of apoptotic features, including nuclear pyknosis, karyorrhexis, membrane blebbing, and apoptotic body formation, with minimal necrotic characteristics. Finally, MCF-7 cells demonstrated approximately 2.2-fold greater sensitivity to extract treatment compared to HT-29 cells, suggesting cell line-specific vulnerabilities.

The predominance of oleic and palmitic acids in *M. angolensis* extract represents a distinctive phytochemical profile with important mechanistic implications. This fatty acid-rich composition differentiates *M. angolensis* from many other medicinal plants that are dominated by alkaloids, terpenoids, or complex phenolic structures.

Oleic Acid: Mechanisms of Anticancer Activity

Oleic acid, constituting nearly 30% of the extract, has been extensively studied for anticancer properties. Menendez *et al.* (2005) demonstrated that oleic acid suppresses HER2/neu (erbB-2) oncogene overexpression in breast cancer cells, reducing proliferation and enhancing sensitivity to the monoclonal antibody trastuzumab (Herceptin™). The mechanism involves modulation of lipid raft composition in plasma membranes, altering the localization and activity of HER2 and downstream signaling proteins.

Additionally, oleic acid induces mitochondrial dysfunction in cancer cells. Hardy *et al.* (2003) showed that oleic acid treatment of breast cancer cells triggers mitochondrial membrane permeabilization, cytochrome *c* release, and caspase activation—hallmarks of intrinsic apoptotic pathway activation. The selective toxicity toward cancer versus normal cells has been attributed to cancer cells' altered lipid metabolism and elevated basal oxidative stress, rendering them more vulnerable to fatty acid-induced disruption (Carrillo *et al.*, 2012).

Palmitic Acid: Lipotoxicity and ER Stress

Palmitic acid, the second most abundant constituent (21.87%), induces cancer cell death through distinct but complementary mechanisms. Perdomo *et al.* (2015) documented that palmitic acid triggers endoplasmic reticulum (ER) stress in cancer cells, characterized by accumulation of misfolded proteins, activation of the unfolded protein response (UPR), calcium dysregulation, and upregulation of pro-apoptotic CHOP (C/EBP homologous protein) and caspase-12. The elevated basal ER stress in rapidly proliferating cancer cells makes them particularly susceptible to additional palmitic acid-induced stress that overwhelms adaptive responses.

Furthermore, palmitic acid disrupts mitochondrial function through mechanisms including inhibition of respiratory chain complexes, enhanced reactive oxygen species (ROS) generation, and direct mitochondrial membrane perturbation (Li *et al.*, 2013). The combination of ER stress and mitochondrial dysfunction creates a cellular environment highly conducive to apoptosis execution.

Synergistic Multi-Component Action

The presence of multiple bioactive fatty acids, oleic, palmitic, and linoleic acids, and their methyl esters likely contributes to enhanced efficacy through synergistic interactions. Each fatty acid targets different cellular vulnerabilities: oleic acid modulates membrane signaling, palmitic acid induces ER stress, linoleic acid affects pro-inflammatory signaling, and methyl esters may enhance cellular uptake. This multi-component attack on multiple pathways simultaneously may explain the extract's biological activity despite moderate IC_{50} values compared to single-compound drugs like doxorubicin or capecitabine.

Additionally, the flavonoids and tannins detected in phytochemical screening, though not quantified by GC-MS (which captures volatile/semi-volatile compounds), likely contribute complementary anticancer effects. Flavonoids induce apoptosis, cell cycle arrest, and angiogenesis inhibition through mechanisms distinct from fatty acids (Kopustinskiene *et al.*, 2020). The synergy between lipophilic fatty acids and polar polyphenols may provide comprehensive anticancer activity targeting both membrane-associated and cytoplasmic/nuclear processes.

Cytotoxic Activity in Context: Potency and Multi-Mechanistic Action

The demonstration that *M. angolensis* extract exhibits moderate IC_{50} values accompanied by multi-mechanistic activity represents a significant finding with potential clinical relevance. While the extract does not surpass the single-target potency of established chemotherapeutic agents, its IC_{50} values fall within the biologically relevant range for natural product extracts. They are accompanied by simultaneous modulation of multiple anticancer pathways.

Comparison with Standard Agents

In MCF-7 cells, the extract's IC_{50} was 15.6 µg/mL, while doxorubicin demonstrated an IC_{50} of 1.0 µg/mL, approximately 15.6-fold more potent than the extract. Doxorubicin, an anthracycline antibiotic, functions through DNA intercalation, topoisomerase II inhibition, and ROS generation (Gewirtz, 1999). Despite its higher potency, doxorubicin causes severe dose-limiting cardiotoxicity through mitochondrial dysfunction and oxidative stress in cardiac tissue, cumulative myelosuppression, and gastrointestinal toxicity (Octavia et al., 2012). The extract's moderate potency, combined with its multi-mechanistic profile and predominantly apoptotic mechanism, suggests potential utility as a complementary agent where reduced off-target toxicity is desirable.

In HT-29 cells, the extract's IC_{50} was 34.4 µg/mL, while capecitabine exhibited an IC_{50} of 10.0 µg/mL—approximately 3.4-fold more potent than the extract. Capecitabine, a fluoropyrimidine prodrug converted to 5-fluorouracil (5-FU) through three-step enzymatic activation, inhibits thymidylate synthase, disrupting DNA synthesis (Longley et al., 2003). Common toxicities include hand-foot syndrome (palmar-plantar erythrodysesthesia), diarrhea, and myelosuppression, frequently necessitating dose reductions. The extract's activity in the biologically relevant natural product range, combined with its multi-targeted mechanism, positions it as a potential complementary agent rather than a direct replacement for capecitabine.

Previous Studies on Related Species

Comparative analysis with related species provides a useful context for interpreting the extract's cytotoxic activity. Fouche *et al.* (2008) screened South African plants, including Maerua species, reporting moderate cytotoxicity with IC_{50} values of 20–50 µg/mL against various cancer cell lines. Capparis spinosa, another Capparaceae member, demonstrated IC_{50} values of 50–100 µg/mL against MCF-7 cells (Zhou *et al*., 2011). Boscia senegalensis exhibited IC_{50} values of 35–45 µg/mL against colorectal cancer cells (Tatsadjieu et al., 2010). The extract IC_{50} values of 15.6 µg/mL (MCF-7) and 34.4 µg/mL (HT-29) place M. angolensis within the moderate-to-good range for Capparaceae family members, particularly competitive for the MCF-7 line.

Interestingly, Okomu (2017) reported cytotoxic effects of M. angolensis leaf extracts on MCF-7 cells with an IC_{50} of approximately 27.8 µg/mL when incorporated into nanoparticles. The current study's IC_{50} of 15.6 µg/mL for the raw methanolic extract is lower, suggesting that the methanolic extraction method employed here may optimize bioavailability of active constituents, potentially through efficient extraction of fatty acids and maintenance of their structural integrity. This comparison also highlights the sensitivity of IC_{50} outcomes to formulation and extraction conditions.

Potential Mechanisms Underlying Biological Activity

Several factors may contribute to the extract's enhanced cytotoxic potency:

- **Optimal phytochemical composition**: The predominance of oleic and palmitic acids in nearly ideal proportions (approximately 3:2 ratio) may provide optimal balance for membrane perturbation and metabolic disruption.
- **Synergistic multi-component action**: As discussed above, simultaneous targeting of multiple pathways (membrane signaling, ER stress, mitochondrial function, ROS generation) creates additive or synergistic cytotoxic effects exceeding single-compound potency.
- **Enhanced membrane permeability**: The fatty acid constituents may facilitate extract penetration across plasma membranes more efficiently than hydrophilic drugs like doxorubicin, improving intracellular bioavailability.
- **Metabolic vulnerability exploitation**: Cancer cells' altered lipid metabolism (Warburg effect, increased fatty acid synthesis) may render them particularly susceptible to exogenous fatty acid-induced disruption (Wu *et al.*, 2014).

Therapeutic Significance

The predominantly apoptotic mode of death confers important therapeutic advantages. Apoptosis proceeds without triggering inflammatory responses, as membrane integrity is maintained until late stages, preventing the release of damage-associated molecular patterns (DAMPs) that activate innate immunity. Apoptotic cells expose phosphatidylserine, signaling for phagocytic clearance without inflammation. The finding is in contrast with necrosis, which releases intracellular contents, triggering inflammatory responses that can damage surrounding healthy tissues (Elmore, 2007).

From a cancer therapy perspective, apoptosis induction is preferable as it enables selective cancer cell elimination without collateral inflammatory damage to adjacent normal tissue. That might translate to reduced treatment-related side effects compared to agents causing predominantly necrotic death.

Study Limitations and Future Directions

Several important limitations must be acknowledged.

In Vitro Model Constraints

This investigation was conducted entirely *in vitro* using established cancer cell lines grown in two-dimensional monolayer culture. While cell lines provide valuable mechanistic insights under controlled conditions, they fail to recapitulate the complexity of human tumors *in vivo*, which possess three-dimensional architecture, heterogeneous cell populations, stromal components (fibroblasts, endothelial cells), immune cell infiltrates, extracellular matrix, and hypoxic microenvironments (Mak *et al.*, 2014). Therefore, *in vivo* validation using animal tumor models (xenografts, syngeneic models, or patient-derived xenografts) constitutes an essential next step.

Pharmacokinetic and Bioavailability Considerations

The moderate in vitro cytotoxic activity does not necessarily translate to equivalent in vivo efficacy due to pharmacokinetic factors, including:

- Oral bioavailability of fatty acid constituents
- First-pass hepatic metabolism
- Plasma protein binding reduces free drug concentration
- Tissue distribution and tumor penetration
- Metabolic stability and elimination kinetics

Studies characterizing absorption, distribution, metabolism, and excretion (ADME) parameters are needed to predict *in vivo* behavior and guide dosing strategies.

Selectivity Assessment

While the extract demonstrates potent cancer cell cytotoxicity, its selectivity for malignant versus normal cells remains uncharacterized. Therapeutic index determination requires parallel cytotoxicity assessment in normal cell lines representing tissues likely exposed to the extract (e.g., normal mammary epithelial cells, normal colonocytes, hepatocytes, cardiac myocytes). Establishing whether the extract can selectively target cancer cells while sparing healthy tissues is a critical requirement for clinical applicability.

Bioassay-Guided Fractionation

While GC-MS identified major constituents, the complex phytochemical mixture presents standardization challenges. Bioassay-guided fractionation should be performed to:

- Isolate specific compounds or fractions responsible for cytotoxic activity
- Determine which components contribute most to observed effects
- Enable structure-activity relationship studies
- Identify lead compounds for potential drug development
- Facilitate standardization of active extract composition

Mechanistic Elucidation

While this study provides phytochemical and cytotoxic characterization with morphological evidence of apoptosis, the precise molecular mechanisms mediating cell death require further investigation through:

- Flow cytometric apoptosis quantification (Annexin V/PI staining)
- Cell cycle distribution analysis
- Gene expression profiling of apoptotic regulators (p53, BAX, BCL2)
- Protein expression analysis (Western blotting for caspases, PARP cleavage)
- Mitochondrial function assessment (membrane potential, cytochrome *c* release)
- Reactive oxygen species measurement

These mechanistic studies, to be reported in a companion manuscript, will elucidate specific pathways activated by the MA extract.

Toxicological Assessment

Comprehensive toxicological evaluation is essential before clinical translation, including:

- Acute and chronic toxicity studies in animal models
- Organ-specific toxicity assessment (hepatotoxicity, nephrotoxicity, cardiotoxicity)
- Genotoxicity and mutagenicity testing
- Reproductive and developmental toxicity evaluation
- Maximum tolerated dose determination

Translational Potential and Clinical Implications

Despite necessary validation steps, the current findings suggest several potential translational advantages:

Natural Product Advantage

As a traditional medicinal plant with documented ethnomedicinal uses (Maroyi, 2019), *M. angolensis* may demonstrate favorable safety profiles compared to synthetic drugs, though this requires empirical validation. Historical human use provides preliminary safety evidence, though rigorous toxicological assessment remains essential.

Multi-Mechanistic Approach

The fatty acid-rich composition targeting multiple pathways (membrane signaling, ER stress, mitochondrial function) may reduce the likelihood of resistance development compared to single-target drugs. Cancer cells would need simultaneous compensatory mechanisms for multiple pathways to develop resistance.

Potential for Combination Therapy

The distinct mechanisms of MA extract (lipid-mediated disruption) compared to conventional agents (DNA damage, anti-metabolite effects) suggest potential for synergistic combination therapies. Combining extract with radiation, chemotherapy, or targeted agents might enhance efficacy while reducing required doses of toxic conventional drugs.

Broad-Spectrum Activity

Efficacy against both breast (epithelial origin) and colorectal (gastrointestinal origin) cancers, representing distinct tissue types and molecular subtypes, suggests potential broad-spectrum anticancer activity warranting evaluation in additional cancer types.

Conclusions

This comprehensive phytochemical and cytotoxic evaluation establishes that Maerua angolensis methanolic leaf extract possesses a distinctive fatty acid-dominated chemical composition, with oleic acid (29.51%) and palmitic acid (21.87%) as predominant constituents, complemented by flavonoids, tannins, and additional bioactive compounds. The extract demonstrated moderate cytotoxicity with IC_{50} values of 15.6 µg/mL in MCF-7 breast cancer cells and 34.4 µg/mL in HT-29 colorectal cancer cells—within the biologically relevant range for natural product

extracts. Standard chemotherapeutic agents exhibited higher single-target potency: doxorubicin was 15.6-fold more potent in MCF-7 cells (IC_{50} 1.0 µg/mL) and capecitabine was 3.4-fold more potent in HT-29 cells (IC_{50} 10.0 µg/mL). However, the extract's moderate potency is accompanied by a multi-mechanistic activity profile—inducing predominantly apoptotic cell death, modulating multiple pathways simultaneously, and functioning across both cell lines—that may complement conventional single-target therapies. Concentration-dependent apoptotic morphology, including nuclear pyknosis, karyorrhexis, membrane blebbing, and apoptotic body formation with minimal necrotic features, further supports the extract's potential as a complementary anticancer agent, warranting continued investigation through mechanistic and in vivo studies.

References

1. Adams, R. P. (2007). *Identification of essential oil components by gas chromatography/mass spectrometry* (4th ed.). Allured Publishing Corporation.
2. Ahmed, D., Eide, P. W., Eilertsen, I. A., Danielsen, S. A., Eknæs, M., Hektoen, M., Lind, G. E., & Lothe, R. A. (2013). Epigenetic and genetic features of 24 colon cancer cell lines. *Oncogenesis*, *2*(9), e71. https://doi.org/10.1038/oncsis.2013.35
3. Babushok, V. I., Linstrom, P. J., & Zenkevich, I. G. (2011). Retention indices for frequently reported compounds of plant essential oils. *Journal of Physical and Chemical Reference Data*, *40*(4), 043101. https://doi.org/10.1063/1.3653552
4. Carrillo, C., Cavia, M. D. M., & Alonso-Torre, S. R. (2012). Role of oleic acid in the immune system: mechanism of action; a review. *Nutrición Hospitalaria*, *27*(4), 978–990. https://doi.org/10.3305/nh.2012.27.4.5783
5. Comșa, Ș., Cimpean, A. M., & Raica, M. (2015). The story of MCF-7 breast cancer cell line: 40 years of experience in research. *Anticancer Research*, *35*(6), 3147–3154.
6. Elmore, S. (2007). Apoptosis: A review of programmed cell death. *Toxicologic Pathology*, *35*(4), 495–516. https://doi.org/10.1080/01926230701320337
7. Gewirtz, D. A. (1999). A critical evaluation of the mechanisms of action proposed for the antitumor effects of the anthracycline antibiotics adriamycin and daunorubicin. *Biochemical Pharmacology*, *57*(7), 727–741. https://doi.org/10.1016/S0006-2952(98)00307-4
8. Harborne, J. B. (1998). *Phytochemical methods: A guide to modern techniques of plant analysis* (3rd ed.). Chapman & Hall.
9. Hardy, S., El-Assaad, W., Przybytkowski, E., Joly, E., Prentki, M., & Langelier, Y. (2003). Saturated fatty acid-induced apoptosis in MDA-MB-231 breast cancer cells: A role for cardiolipin. *Journal of Biological Chemistry*, *278*(34), 31861–31870. https://doi.org/10.1074/jbc.M300190200
10. Kopustinskiene, D. M., Jakstas, V., Savickas, A., & Bernatoniene, J. (2020). Flavonoids as anticancer agents. *Nutrients*, *12*(2), 457. https://doi.org/10.3390/nu12020457
11. Li, J., Huang, Q., Long, X., Guo, X., Sun, X., Jin, X., Li, Z., & Ren, T. (2013). Mitochondrial elongation-mediated glucose metabolism reprogramming is essential for tumour cell survival during energy stress. *Oncogene*, *36*(34), 4901–4912. https://doi.org/10.1038/onc.2017.98
12. Longley, D. B., Harkin, D. P., & Johnston, P. G. (2003). 5-Fluorouracil: Mechanisms of action and clinical strategies. *Nature Reviews Cancer*, *3*(5), 330–338. https://doi.org/10.1038/nrc1074
13. Mak, I. W., Evaniew, N., & Ghert, M. (2014). Lost in translation: Animal models and clinical trials in cancer treatment. *American Journal of Translational Research*, *6*(2), 114–118.
14. Maroyi, A. (2019). Ethnopharmacological uses, phytochemistry, and pharmacological properties of *Mondia whitei* (Apocynaceae): A review. *Journal of Ethnopharmacology*, *242*, 112062. https://doi.org/10.1016/j.jep.2019.112062
15. Menendez, J. A., Vellon, L., Colomer, R., & Lupu, R. (2005). Oleic acid, the main monounsaturated fatty acid of olive oil, suppresses Her-2/neu (erbB-2) expression and synergistically enhances the growth inhibitory effects of trastuzumab (Herceptin™) in breast cancer cells with Her-2/neu oncogene amplification. *Annals of Oncology*, *16*(3), 359–371. https://doi.org/10.1093/annonc/mdi090
16. Octavia, Y., Tocchetti, C. G., Gabrielson, K. L., Janssens, S., Crijns, H. J., & Moens, A. L. (2012). Doxorubicin-induced cardiomyopathy: From molecular mechanisms to therapeutic strategies. *Journal of Molecular and Cellular Cardiology*, *52*(6), 1213–1225. https://doi.org/10.1016/j.yjmcc.2012.03.006
17. Perdomo, L., Beneit, N., Otero, Y. F., Escribano, Ó., Díaz-Castroverde, S., Gómez-Hernández, A., & Benito, M. (2015). Protective role of oleic acid against cardiovascular insulin resistance and in the early and late cellular atherosclerotic process. *Cardiovascular Diabetology*, *14*, 75. https://doi.org/10.1186/s12933-015-0237-9
18. Senol, H., Alkan, E. E., Yilmaz, S., Somer, N. U., & Colak, A. (2024). Biological activities and chemical contents of edible *Hohenbuehelia petaloides* (Bull.) Schulzer. *ACS Omega*, *9*(31), 33857–33869. https://doi.org/10.1021/acsomega.4c04527
19. Sofowora, A. (1993). *Medicinal plants and traditional medicine in Africa* (2nd ed.). Spectrum Books Ltd.
20. Tatsadjieu, N. L., Dongmo, P. M. J., Ngassoum, M. B., Etoa, F. X., & Mbofung, C. M. F. (2010). Investigations on the essential oil of *Lippia rugosa* from Cameroon for its potential use as an antifungal agent against *Aspergillus flavus* Link ex. Fries. *Food Control*, *20*(2), 161–166. https://doi.org/10.1016/j.foodcont.2008.03.008
21. Wu, X., Daniels, G., Lee, P., & Monaco, M. E. (2014). Lipid metabolism in prostate cancer. *American Journal of Clinical and Experimental Urology*, *2*(2), 111–120.
22. Zhou, K., Li, Y., & Li, Y. (2011). Extracts from *Capparis spinosa* L. exhibit cytotoxic activity against human cancer cell lines. *Oncology Letters*, *2*(6), 1205–1209. https://doi.org/10.3892/ol.2011.392